Available online at www.sciencedirect.com
ScienceDirect
Bioorganic & Medicinal Chemistry Letters 18 (2008) 923–928
Bioorganic & Medicinal Chemistry Letters

# The discovery of odanacatib (MK-0822), a selective inhibitor of cathepsin K

Jacques Yves Gauthier,[a] Nathalie Chauret,[a] Wanda Cromlish,[a] Sylvie Desmarais,[a] Le T. Duong,[b] Jean-Pierre Falgueyret,[a] Donald B. Kimmel,[b] Sonia Lamontagne,[a] Serge Léger,[a] Tammy LeRiche,[a] Chun Sing Li,[a] Frédéric Massé,[a] Daniel J. McKay,[a] Deborah A. Nicoll-Griffith,[a] Renata M. Oballa,[a] James T. Palmer,[c] M. David Percival,[a] Denis Riendeau,[a] Joel Robichaud,[a] Gideon A. Rodan,[b] Sevgi B. Rodan,[b] Carmai Seto,[a] Michel Thérien,[a] Vouy-Linh Truong,[a] Michael C. Venuti,[c] Gregg Wesolowski,[b] Robert N. Young,[a] Robert Zamboni[a] and W. Cameron Black[a,*]

[a]*Merck Frosst Centre for Therapeutic Research, 16711 TransCanada Hwy, Kirkland, Que., Canada H9H 3L1*
[b]*Department of Bone Biology and Osteoporosis, Merck Research Laboratories, West Point, PA 19846, USA*
[c]*Celera Genomics, Inc., 180 Kimball Way, South San Francisco, CA 94080, USA*

Received 8 November 2007; revised 17 December 2007; accepted 19 December 2007
Available online 15 January 2008

Dedicated to the memory of Dr. Gideon Rodan, deceased, January 1, 2006

**Abstract**—Odanacatib is a potent, selective, and neutral cathepsin K inhibitor which was developed to address the metabolic liabilities of the Cat K inhibitor L-873724. Substituting P1 and modifying the P2 side chain led to a metabolically robust inhibitor with a long half-life in preclinical species. Odanacatib was more selective in whole cell assays than the published Cat K inhibitors balicatib and relacatib. Evaluation in dermal fibroblast culture showed minimal intracellular collagen accumulation relative to less selective Cat K inhibitors.


Cathepsin K (Cat K) is a lysosomal cysteine protease that is highly expressed in osteoclasts, the cells responsible for bone degradation during bone remodeling. Type I collagen is a major component of bone and Cat K has high collagenase activity, particularly at the acidic pH that is required to dissolve the calcium hydroxyapatite component of bone. Emerging evidence that Cat K is the primary enzyme involved in osteoclastic bone resorption has made it an important target for the treatment of osteoporosis.[1] Several studies have shown that Cat K deficiency leads to an increase in bone mineral density (BMD).[2] Pharmacological studies of Cat K inhibitors in rats[3] and monkeys[4] have shown reductions in biochemical markers of bone resorption and

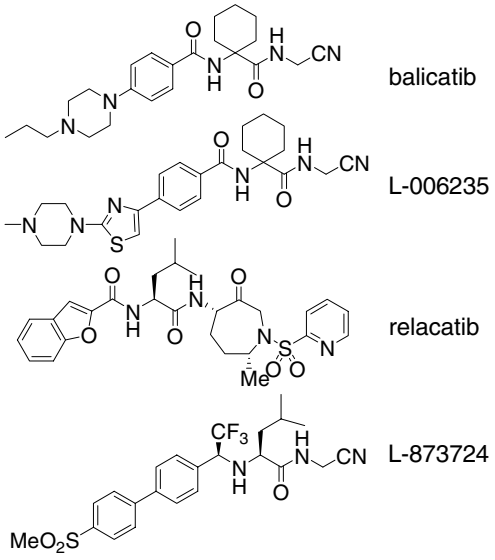


**Figure 1.** Published Cat K inhibitors.

*Keywords*: Cathepsin K; Cysteine protease; Odanacatib; MK-0822; Osteoporosis.
* Corresponding author. Tel.: +1 514 428 3073; fax: +1 514 428 4900; e-mail: blackc@merck.com

0960-894X/$ - see front matter © 2008 Elsevier Ltd. All rights reserved.
doi:10.1016/j.bmcl.2007.12.047

increased BMD. Recently, clinical data have been disclosed for the Cat K inhibitor balicatib (Fig. 1), demonstrating a reduction of biochemical markers of bone resorption and increases in BMD over 1 year of treatment.[5]

We have previously reported on our effort to identify potent and selective inhibitors of Cat K.[6] Our initial proof-of-concept compound, L-006235, was highly selective over cathepsins B, L, and S in enzyme assays and had good pharmacokinetics.[7] However more detailed studies revealed that the selectivity profile ns was severely eroded in more physiologically relevant cell-based enzyme occupancy assays.[8] The relevance of these data was demonstrated in a Cat S-dependent B cell line assay in which L-006235 blocked antigen presentation. This loss of selectivity in cell-based assays can be explained by the lysosomotropic properties of these basic, lipophilic compounds. Since off-target cathepsins are found in lysosomes (pH 4–5), the lysosomal accumulation of a basic Cat K inhibitor results in an apparent increase in potency on these anti-targets. High selectivity will be important to the success of a development candidate, precluding the use of a basic moiety in inhibitor design.

Balicatib is structurally related to L-006235 and is also lysosomotropic.[8] Whole cell assays showed poor selectivity as was observed for L-006235. Recently it was announced that the Phase II development of balicatib has been discontinued due to skin rash and rarer incidences of morphea-like skin changes.[9] Another Cat K inhibitor in clinical development, relacatib, is non-basic and therefore not lysosomotropic, but has poor selectivity over cathepsins B, L, S, and V in enzyme assays.[10]

Our initial attempts to remove the basic substituent in P3 led to Cat K inhibitors with poor activity, selectivity, and pharmacokinetic properties. The loss in activity was attributed to the loss of a beneficial ionic interaction between the charged amine and $Asp^{61}$ in the S3 pocket.[7] Since this residue is absent in the off-target cathepsins, the potencies against the anti-targets were not dramatically affected and selectivity was consequently reduced. Replacing the P2 amide bond with a trifluoroethylamine provided a 10- to 20-fold increase in potency on Cat K.[11] Using this motif, neutral inhibitors with high potency and selectivity were prepared. L-873724 was identified as a 0.2 nM Cat K inhibitor with >800-fold selectivity over other cathepsins. In vivo studies showed that this neutral Cat K inhibitor suppressed biochemical markers of bone resorption in a rhesus monkey model.[12]

L-873724 has metabolic liabilities that prevented its further development. An analysis of its metabolic profile provided guidance for addressing these liabilities. Subsequent blocking of the key metabolic sites resulted in the identification of odanacatib (MK-0822) which is currently in clinical development.

The pharmacokinetics of L-873724 in rat, dog, and monkey have been reported.[12] The short half-life (2 h) and clearance (Cl = 7.5 mL/min/kg) in monkey raised concerns that this compound may not be suitable for once-daily dosing in humans. Incubations in human hepatocytes showed that the major route of metabolism was hydroxylation on the methine of the leucine side chain (**1**)[13] as shown in Scheme 1. A minor pathway leading to the hydrolysis of the P1 amide bond (**2**) was also observed. Analysis of plasma from several species showed several circulating metabolites. In particular, the lactone **3** was found to be circulating at high levels in rhesus monkey (10× L-873724 concentration at 8 h) even though it was only a minor component in rat plasma. To understand the potential relevance of this metabolite to humans, a synthetic standard of **3** was incubated in fresh plasma from rat, rhesus monkey, and human. In all three species, the lactone hydrolyzed to hydroxyacid **4** over the course of the incubation (37 °C, 1 h). However this hydrolysis was much more efficient in rat plasma (50% conversion) than in rhesus monkey plasma (5% conversion). The extent of hydrolysis in human plasma was intermediate (28–40% conversion) leading us to conclude that this metabolite would likely circulate in humans.

Further investigations revealed that the leucine hydroxylation occurred exclusively due to CYP3A activity. Adding the CYP3A inhibitor ketoconazole to the hepatocyte incubations resulted in a near-complete blockade of metabolism. When L-873724 was incubated for 1 h in pooled human microsomes, only a 10% recovery of the parent drug was observed. Microsomal incubation in the presence of a CYP3A inhibitory antibody gave >90% recovery of parent drug. Finally, incubation with several recombinant CYPs (1A1, 2D6*1, 3A4, 2C9*1, 2C9*2, 2C9*3, and 2C19) showed that only CYP3A led to detectable metabolite formation. Metabolism by only CYP3A can lead to variable exposure when co-dosed with other drugs that are CYP3A inhibitors and inducers.

To address the metabolic liabilities listed above, both the P1 and P2 residues were modified to minimize leucine hydroxylation, amide hydrolysis, and lactonization (Table 1). Most P1 substituents resulted in a loss of activity. One of the more active compounds (**14**) was provided by incorporation of an (*S*)-benzyl group, but the corresponding increase in potency on cathepsins B, L, and S resulted in a poor selectivity profile. The (*R*)-

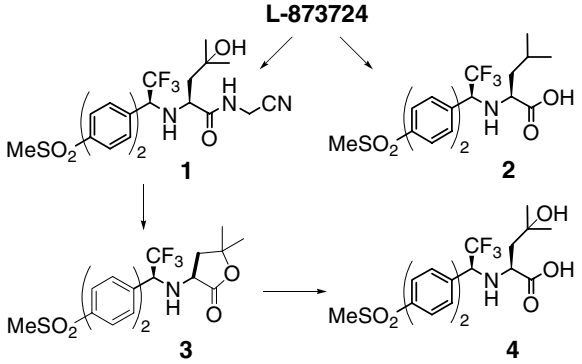


**Scheme 1.** Metabolic pathways for L-873724 based on in vitro and in vivo studies.

**Table 1.** In vitro activity of L-873724 analogues with P1 substitution and stabilized P2 groups

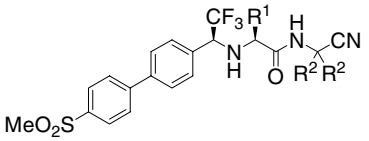

| Compound | $R^1$ | $R^2$ | $IC_{50}$[a] (nM) | | | |
|---|---|---|---|---|---|---|
| | | | Cat K[b] | Cat B | Cat L | Cat S |
| L-873724 | *i*-Bu | H, H | 0.2 | 5239 | 264 | 178 |
| **12** | *i*-Bu | (*S*)-Me, H | 1.2 | >10,000 | 3389 | 2237 |
| **13** | *i*-Bu | (*R*/*S*)-Ph, H | 0.6 | 3453 | 667 | 217 |
| **14** | *i*-Bu | (*S*)-Bn, H | 0.6 | 953 | 67 | 38 |
| **15** | *i*-Bu | (*R*)-Bn, H | 5.1 | >10,000 | 2940 | 2834 |
| **16** | *i*-Bu | 1,1-$Me_2$ | 4.0 | >10,000 | >10,000 | 2489 |
| **17** | *i*-Bu | 1,1-cPr | 0.3 | >10,000 | 456 | 266 |
| **18** | *i*-Bu | 1,1-cBu | 16 | >10,000 | >10,000 | >10,000 |
| **19** | 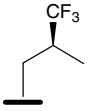 | 1,1-cPr | 0.3 | >10,000 | 262 | 56 |
| **20** | 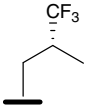 | 1,1-cPr | 0.4 | >10,000 | 2650 | 170 |
| **21** | 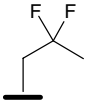 | 1,1-cPr | 0.2 | 100 | 472 | 17 |
| **22** | 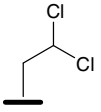 | 1,1-cPr | <0.2 | 1528 | 110 | 15 |
| **23** | 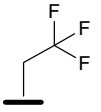 | 1,1-cPr | 1.5 | 434 | 750 | 89 |
| **24** (odanacatib) | 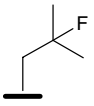 | 1,1-cPr | 0.2 | 1034 | 2995 | 60 |

[a] $IC_{50}$ values represent an average of at least three titrations. Standard deviations for these assays were typically within 35% of the $IC_{50}$ values.
[b] Humanized rabbit Cat K (Ref. 6); others are human enzymes. See Ref. 17 for assay conditions.

benzyl group provided a compound (**15**) that is 8-fold less potent, suggesting that there is limited space for substituents in the back of the P1 pocket. The gem-dimethyl substituted **16** shows similar behavior. The optimal substituent was a 1,1-cyclopropane ring (**17**) which gave an in vitro profile similar to that of the unsubstituted aminonitrile. Increasing the ring size to a 1,1-cyclobutane substituent (**18**) resulted in a 50-fold loss in potency, again demonstrating the restrictions of the P1 pocket.

Previous SAR studies of cathepsin inhibitors have shown that the P2 substituent is critical to achieving both potency and selectivity.[7] For Cat K, an isobutyl substituent in P2 has been found to provide an optimal in vitro profile. The metabolic liability of this group led us to attempt metabolic stabilization by introducing halogens in various locations. Even though the steric differences of the resulting inhibitors are subtle, the impact on both Cat K potency and selectivity is significant (Table 1). For example, the two diastereomers **19** and **20**, while having similar potency on Cat K, show a 10-fold difference in Cat L potency. The difluoropropyl side chain **21** has similar potency on Cat K, but has poor selectivity on Cat B, L, and S. The dichloroethyl side chain **22** has increased potency against all the tested cathepsins, while the trifluoroethyl derivative **23** loses activity on Cat K, but gains activity on Cat B. The optimal combination of potency and selectivity was found with the 4-fluoroleucine derivative **24** (odanacatib, MK-0822). It was particularly gratifying to note that this compound had little activity on Cat L, since the Cat L−/− mouse shows several undesirable phenotypes.[14] Evaluation against other cathepsins gave $IC_{50}$s of 795 nM versus Cat F and 762 nM versus Cat V. There

was no measurable activity versus cathepsins C, H, and Z (>10 μM). Odanacatib is a reversible inhibitor of Cat K with on- and off-rates of $5.3 \times 10^6\ M^{-1}\ s^{-1}$ and $0.0008\ s^{-1}$ ($t_{1/2} \sim 14$ min), respectively.

The inhibitors described above were prepared according to methods analogous to those published previously.[12] The route is exemplified by the synthesis of odanacatib (**24**) in Scheme 2. The synthesis of 4-fluoroleucinol begins with commercially available aspartic acid derivative **5**. Reduction of the acid followed by activation with tosic anhydride provides the cyclic carbamate **6**. Methyl Grignard addition to the benzyl ester and fluorination of the resulting tertiary alcohol gave fluoride **7**. Carbamate hydrolysis with barium hydroxide proceeded in quantitative yield and the resulting amino alcohol was silylated to facilitate isolation and provide stereochemical control in the subsequent imine addition step. Condensation of **8** with trifluoroacetaldehyde hemiacetal provided imine **9** which was treated with bromophenyllithium to give the trifluoroethylamine in a 10:1 ratio of *S*,*S* to *R*,*S* diastereomers. Desilylation followed by periodic acid oxidation[15] under anhydrous conditions gave the carboxylic acid which was crystallized as the dicyclohexylamine salt to give >99% de. Amide formation with cyclopropaneaminoacetonitrile proceeded using HATU to provide **11**. Suzuki coupling followed by sulfide oxidation then provided odanacatib **24**. The P2 amino acids and aminoalcohols required for analogues **19**–**23** were prepared according to literature methods and converted into final products as described in Scheme 2. Details are provided in Supplementary material. Additional synthetic routes to this class of compounds have been reported.[16]

The potency of odanacatib was evaluated in a functional bone resorption assay using rabbit osteoclasts cultured on bovine bone. Since the majority of our Cat K inhibitors are less potent on rabbit Cat K than on human Cat K, a 'corrected bone res' value has been calculated based on the difference between the rabbit and human potencies (Table 2). This allows comparisons of functional potency to be made between compounds in a human context. Odanacatib showed potency similar to L-873724 and was 3- to 4-fold more potent than balicatib and relacatib. The reduced potency of inhibitors in this assay relative to the Cat K enzyme assay may reflect the high fractional inhibition of Cat K required to inhibit bone resorption in osteoclasts.

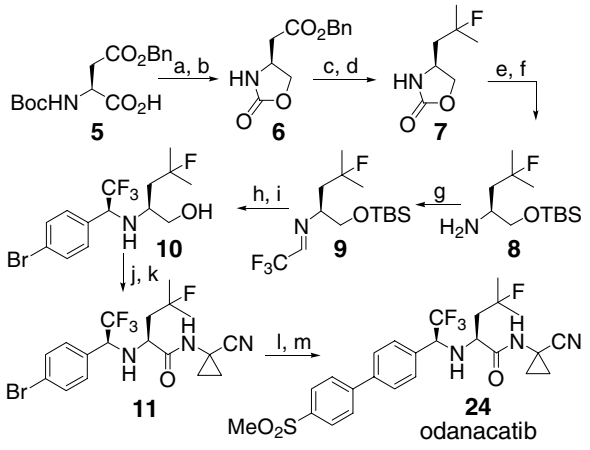


**Scheme 2.** Reagents and conditions: (a) ClCOOiBu, NMM, $NaBH_4$, DME, 85%; (b) $Ts_2O$, pyr, dichloroethane, 83%; (c) MeMgBr, toluene/THF, 85%; (d) DAST, $CH_2Cl_2$, 60%; (e) $Ba(OH)_2$, $EtOH/H_2O$, 100%; (f) TBSCl, $Et_3N$; (g) $CF_3C(OH)OEt$, PhH, 88% (two steps); (h) BrPhLi, THF; (i) TBAF, THF, 75% (two steps); (j) $H_5IO_6$, $CrO_3$, $CH_3CN$, 60%; (k) 1-amino-1-cyanocyclopropane hydrochloride, *i*-$Pr_2NEt$, HATU, DMF, 80%; (l) $MeSPhB(OH)_2$, $PdCl_2dppf$, $Na_2CO_3$, DMF, 70%; (m) $H_2O_2$, $Na_2WO_42H_2O$, $Bu_4NHSO_4$, EtOAc, 97%.

Odanacatib was evaluated in whole cell enzyme occupancy assays using human HepG2 cells (Cat B, L) and Ramos cells (Cat S) for selectivity versus off-target cathepsins (Table 3) as previously described.[17] In these whole cell assays, odanacatib showed similar potencies to those obtained in the corresponding purified enzyme assays. This provided a high degree of selectivity versus the corrected bone res Cat K assay, particularly compared to the other catibs. The lowest selectivity of odanacatib is against Cat S, so its potential to inhibit Cat S in vitro was addressed with two functional assays. Odanacatib was a weak inhibitor of antigen presentation, measured in a mouse B cell line ($IC_{50} = 1.5 \pm 0.4$ μM), compared to the Cat S inhibitor LHVS ($IC_{50} = 0.001$ μM) in the same assay.[8] Odanacatib also showed weak inhibition of the processing of the MHC II invariant chain protein Iip10 in mouse splenocytes compared to LHVS (minimum inhibitory concentration 1–10 μM versus 0.01 μM, respectively).[18] The potency of odanacatib is 4-fold greater against isolated mouse Cat S than human Cat S, therefore the potential for Cat S mediated immunosuppression appears to be low.

Cathepsins B, K, L, S, and V are all expressed in skin tissue and have some ability to degrade collagen and

**Table 2.** Cat K enzyme activity and functional bone resorption assay

| Compound | $IC_{50}$ (nM) | | | |
|---|---|---|---|---|
| | Human Cat K | Rabbit Cat K | Rabbit Bone Res[a] | 'Corrected' Bone Res[c] |
| L-873724 | 0.2 | 0.8 | 13 ± 1 | 3 |
| Odanacatib | 0.2 | 1.0 | 23 ± 6 | 5 |
| Balicatib | 0.6 | 2.7 | 97 ± 13 | 22 |
| Relacatib | 0.5[b] | 0.5 | 15 ± 2 | 15 |

[a] $IC_{50}$ values represent an average of at least three titrations ± SEM.
[b] Humanized rabbit Cat K.
[c] Bone res $IC_{50} \times$ hCat K $IC_{50}$/rabCat K $IC_{50}$.

**Table 3.** Whole cell potency on cathepsins K, B, L, and S

| Compound | $IC_{50}$ (nM) | | | |
|---|---|---|---|---|
| | Cat K 'Corrected' Bone Res | Enzyme occupancy | | |
| | | Cat B (HepG2) | Cat L (HepG2) | Cat S (Ramos) |
| L-873724 | 3 | 4807 | 1221 | 95 |
| Odanacatib | 5 | 1050 | 4843 | 45 |
| Balicatib | 22 | 61 | 48 | 2900 |
| Relacatib | 15 | 14 | 2 | 8 |

extracellular matrix. A key pathway for collagen degradation by fibroblasts involves MMP-dependent partial digestion and phagocytosis, followed by cysteine cathepsin-dependent intracellular degradation.[19,20] We hypothesized that the fibrotic events caused by balicatib[9] are due to inhibition of multiple cathepsins by virtue of its lysosomotropic nature, resulting in a build up of matrix. A cellular model was used in which primary human dermal fibroblasts (HDF) were cultured in 3-D collagen gel and inhibitors added for the final 3 days.[21] The cells were removed from the collagen by collagenase treatment, fixed and permeabilized, and intracellular type I collagen detected using an anti-type I collagen mAb and a FITC-labeled $2^{o}$Ab with quantitation by flow cytometry (see Supplementary material). Balicatib and the non-selective cathepsin inhibitors relacatib (Fig. 2) and E64/E64d (data not shown) caused a 3- to 7-fold accumulation of intracellular Type I collagen in HDF at concentrations of 1–10 μM. In contrast, an inactive structural analogue of balicatib (compound **2** in Ref. 8) and an inactive diastereomer of relacatib (compound **13** in Ref. 10) showed less than 1.5-fold accumulation of collagen at concentrations up to 10 μM (data not shown). The high degree of cellular selectivity of odanacatib was again demonstrated by its minimal effect on collagen accumulation, even at the relatively high concentration of 10 μM (Fig. 2).

Odanacatib exhibited excellent metabolic stability in hepatocyte incubations across several species. In standard incubations ($2 \times 10^6$ cells/mL, 20 μM, 2 h), a 96% recovery of parent was found in rat hepatocytes and a 98% recovery was obtained in rhesus monkey hepatocytes. High recovery (>99%) was observed in both dog and human hepatocyte incubations.

The pharmacokinetics of odanacatib were evaluated in several preclinical species (Table 4). This molecule is highly crystalline with low aqueous solubility, and oral bioavailability was found to be highly dependent on vehicle, dosage, and sample preparation. For example, in the dog, the oral bioavailability when dosed as a suspension in 0.5% methocel was only 6% at 5 mg/kg, but increased to 100% when dosed as an amorphous dispersion prepared by adding a PEG-200 solution of the compound to methocel with sonication. Similarly, the bioavailability in rats when dosed at 5 mg/kg as a solution in PEG-400 was found to be 38%. The half-lives were long in all species and were consistent with the observed metabolic stability.

**Table 4.** Pharmacokinetics of odanacatib (0.5% methocel + 0.2% SDS as oral vehicle)

| Species | po Dose (mg/kg) | %F | Cl (mL/min/kg) | Half-life (h) | Vdss (L/kg) |
|---|---|---|---|---|---|
| Rat | 10 | 8 | 2.0 | 6 | 1.1 |
| Dog | 5 | 6 | 0.13 | 57 | 0.6 |
| Rh. Monk. | 5 | 7 | 6.1 | 18 | 1.6 |

In conclusion, by blocking the sites of metabolism on L-873724, a compound was identified with minimal in vitro metabolism and long half-lives in preclinical species. Odanacatib has greater bone resorption activity and greater selectivity versus off-target cathepsins than do balicatib and relacatib. This reduced activity against other cathepsins may be responsible for the lower level of undesired collagen accumulation in skin fibroblasts compared to balicatib and relacatib. Odanacatib is currently in clinical development for the treatment of postmenopausal osteoporosis.

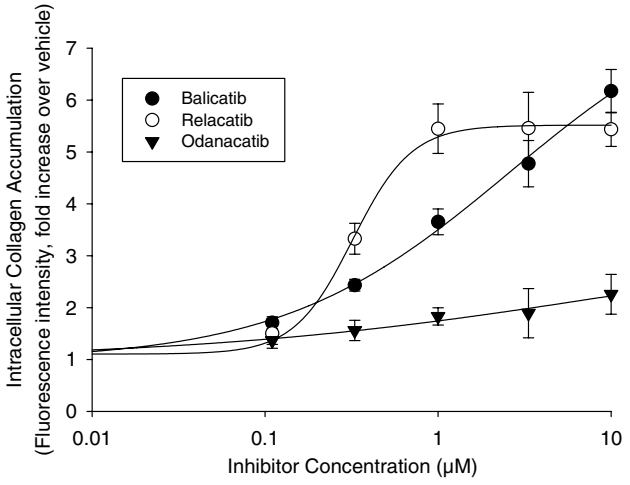


**Figure 2.** Effect of balicatib, relacatib, and odanacatib on the intracellular accumulation of Type I collagen in cultured primary human dermal fibroblasts. The data represent the average ± SD for at least $n = 2$ experiments for each inhibitor. A similar profile was observed using cells from a second donor.

## Supplementary data

Supplementary data associated with this article can be found, in the online version, at doi:10.1016/j.bmcl.2007.12.047.

## References and notes

1. For recent reviews: (a) Grabowska, U. B.; Chambers, T. J.; Shiroo, M. *Curr. Opin. Drug Discovery Dev.* **2005**, *8*, 619; (b) Marquis, R. W. *Ann. Rep. Med. Chem.* **2004**, *39*, 79.
2. Saftig, P.; Hunziker, E.; Wehmeyer, O.; Jones, S.; Boyde, A.; Rommerskirch, W.; Moritz, J. D.; Schu, P.; von Figura, K. *Proc. Natl. Acad. Sci.* **1998**, *95*, 13453.
3. Barrett, D. G.; Boncek, V. M.; Catalano, J. G.; Deaton, D. N.; Hassell, A. M.; Jurgensen, C. H.; Long, S. T.; McFadyen, R. B.; Miller, A. B.; Miller, L. R.; Payne, J. A.; Ray, J. A.; Samano, V.; Shewchuk, L. M.; Tavares, F. X.; Wells-Knecht, K. J.; Willard, D. H., Jr.; Wright, L. L.; Zhou, H. Q. *Bioorg. Med. Chem. Lett.* **2005**, *15*, 3540.
4. Kumar, S.; Dare, L.; Vasko-Moser, J. A.; James, I. E.; Blake, S. M.; Rickard, D. J.; Hwang, S. M.; Tomaszek, T.; Yamashita, D. S.; Marquis, R. W.; Oh, H.; Jeong, J. U.; Veber, D. F.; Gowen, M.; Lark, M. W.; Stroup, G. *Bone* **2007**, *40*, 122.
5. Adami, S.; Supronik, J.; Hala, T.; Brown, J. P.; Garnero, P.; Haemmerle, S.; Ortmann, C. E.; Bouisset, F.; Trechsel, U. *J. Bone Min. Res.* **2006**, *21*, S24.

6. Robichaud, J.; Oballa, R.; Prasit, P.; Falgueyret, J.-P.; Percival, M. D.; Wesolowski, G.; Rodan, S. B.; Kimmel, D.; Johnson, C.; Bryant, C.; Venaktraman, S.; Setti, E.; Mendoca, R.; Palmer, J. T. *J. Med. Chem.* **2003**, *46*, 3709.
7. Palmer, J. T.; Bryant, C.; Wang, D.-X.; Davis, D. E.; Setti, E. L.; Rydzewski, R. M.; Venkatraman, S.; Tian, Z.-Q.; Burrill, L. C.; Mendonca, R. V.; Springman, E.; McCarter, J.; Chung, T.; Cheung, H.; McGrath, M.; Somoza, J.; Enriquez, P.; Yu, Z. W.; Strickley, R. M.; Liu, L.; Venuti, M. C.; Percival, M. D.; Falgueyret, J.-P.; Prasit, P.; Oballa, R.; Riendeau, D.; Young, R. N.; Wesolowski, G.; Rodan, S. B.; Johnson, C.; Kimmel, S. B.; Rodan, G. *J. Med. Chem.* **2005**, *48*, 7520.
8. Falgueyret, J.-P.; Desmarais, S.; Oballa, R.; Black, W. C.; Cromlish, W.; Khougaz, K.; Lamontagne, S.; Massé, F.; Riendeau, D.; Toulmond, S.; Percival, M. D. *J. Med. Chem.* **2005**, *48*, 7535.
9. Adami, S.; Supronik, J.; Hala, T.; Brown, J. P.; Garnero, P.; Haemmerle, S.; Ortmann, C. E.; Bouisset, F.; Trechsel, U. ASBMR 28th Annual Meeting, 2006, Abstract 1085.
10. Yamashita, D. S.; Marquis, R. W.; Xie, R.; Nidamarthy, S. D.; Oh, H. J.; Jeong, J. U.; Erhard, K. F.; Ward, K. W.; Roethke, T. J.; Smith, B. R.; Cheng, H. Y.; Geng, X.; Lin, F.; Offen, P. H.; Wang, B.; Nevins, N.; Head, M. S.; Haltiwanger, R. C.; Narducci Sarjeant, A. A.; Liable-Sands, L. M.; Zhao, B.; Smith, W. W.; Janson, C. A.; Gao, E.; Tomaszek, T.; McQueney, M.; James, I. E.; Gress, C. J.; Zembryki, D. L.; Lark, M. W.; Veber, D. F. *J. Med. Chem.* **2006**, *49*, 1597.
11. Black, W. C.; Bayly, C. I.; Davis, D. E.; Desmarais, S.; Falgueyret, J.-P.; Léger, S.; Li, C. S.; Massé, F.; McKay, D. J.; Palmer, J. T.; Percival, M. D.; Robichaud, J.; Tsou, N.; Zamboni, R. *Bioorg. Med. Chem. Lett.* **2005**, *15*, 4741.
12. Li, C. S.; Deschenes, D.; Desmarais, S.; Falgueyret, J. P.; Gauthier, J. Y.; Kimmel, D. B.; Leger, S.; Masse, F.; McGrath, M. E.; McKay, D. J.; Percival, M. D.; Riendeau, D.; Rodan, S. B.; Therien, M.; Truong, V. L.; Wesolowski, G.; Zamboni, R.; Black, W. C. *Bioorg. Med. Chem. Lett.* **2006**, *16*, 1985.
13. The structures of **1**–**4** were proposed based on mass analysis and confirmed with synthetic standards.
14. (a) Petermann, I.; Mayer, C.; Stypmann, J.; Biniossek, M. L.; Tobin, D. J.; Engelen, M. A.; Dandekar, T.; Grune, T.; Schild, L.; Peters, C.; Reinheckel, T. *FASEB J.* **2006**, *20*, 1256; (b) Nakagawa, T.; Roth, W.; Wong, P.; Nelson, A.; Farr, A.; Deussing, J.; Villadangos, J. A.; Ploegh, H.; Peters, C.; Rudensky, A. Y. *Science* **1998**, *280*, 450.
15. Zhao, M.; Li, J.; Song, Z.; Desmond, R.; Tschaen, D. M.; Grabowski, E. J. J.; Reider, P. J. *Tetrahedron Lett.* **1998**, *39*, 5323.
16. (a) Roy, A.; Gosselin, F.; O'Shea, P. D.; Chen, C.-Y. *J. Org. Chem.* **2006**, *71*, 4320; (b) Hughes, G.; Devine, P. N.; Naber, J. R.; O'Shea, P. D.; Foster, B. S.; McKay, D. J.; Volante, R. P. *Angew. Chem. Int. Ed.* **2007**, *46*, 1839.
17. Falgueyret, J. P.; Black, W. C.; Cromlish, W.; Desmarais, S.; Lamontagne, S.; Mellon, C.; Riendeau, D.; Rodan, S.; Tawa, P.; Wesolowski, G.; Bass, K. E.; Venkatraman, S.; Percival, M. D. *Anal. Biochem.* **2004**, *335*, 218.
18. Ward, Y. D.; Thomson, D. S.; Frye, L. L.; Cywin, C. L.; Morwick, T.; Emmanuel, M. J.; Zindell, R.; McNeil, D.; Bekkali, Y.; Girardot, M.; Hrapchak, M.; DeTuri, M.; Crane, K.; White, D.; Pav, S.; Wang, Y.; Hao, M. H.; Grygon, C. A.; Labadia, M. E.; Freeman, D. M.; Davidson, W.; Hopkins, J. L.; Brown, M. L.; Spero, D. M. *J. Med. Chem.* **2002**, *45*, 5471, Isolated mouse splenocytes were treated with Cat S inhibitors, lysates run on SDS–PAGE followed by Western blot detection of p10 accumulation using a rat-anti-mouse CD74 antibody (Biosciences).
19. Lee, H.; Overall, C. M.; McCulloch, C. A.; Sodek, J. *Mol. Biol. Cell* **2006**, *17*, 4812.
20. Everts, V.; van der Zee, E.; Creemers, L.; Beertsen, W. *Histochem. J.* **1996**, *28*, 229.
21. Nakagawa, S.; Pawelek, P.; Grinnell, F. *J. Invest. Dermatol.* **1989**, *93*, 792.